Chapter IV

Results and Discussion

4.1 Characteristics of Hydroxyapatite

4.1.1 Chemical Analysis of Hydroxyapatite

Quantities of calcium, phosphorus and impurities of MP powder were analysed by XRF-borate fusion method by Mineral Assay and Services. The results of these were shown in Table 4.1. The Ca:P ratio obtained at 1.65 was lower than the stoichiometric one (1.67). It was shown that MP powder was a calcium deficient HAp.

Table 4.1 Chemical analysis of HAp powder

Chemical Composition	Quantity (%)
CaO	54.0
P_2O_5	41.3
Ca:P mole ratio	1.65:1
Impurities	
MgO	1.24
Na_2O	1.22
K_2O	0.02
Fe_2O_3	0.07
MnO	< 0.01
SiO_2	< 0.01
TiO_2	< 0.01
Cr_2O_3	< 0.01
Al_2O_3	< 0.01

4.1.2 Phases Identification

The pattern of crystalline phase of HAp was identified by x-ray diffraction method as shown in Fig 4.1. It exhibited characteristic of HAp pattern with the highest peak at $2\theta = 31.8°$, proved with the diffraction card of HAp. The sharp peaks of XRD indicated the well crystallized state of hydroxyapatite and the second phase was not observed.

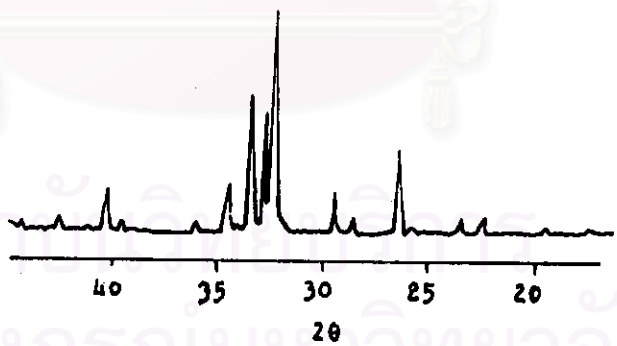

Fig 4.1 XRD patterns of HAp

4.2 Forming and Characteristics of Hydroxyapatite

4.2.1 Forming of Hydroxyapatite

Rod shape specimens of HAp were formed by extrusion process. Generally, extrusion is a plastic forming method but HAp is a low plasticity material so that it was necessary to prepared the appropriate properties of HAp before it was extruded. The involving factors were controlled such as, moisture, pressure, lubricant, binder and blending.

The condition for extruded HAp specimens were shown in Table 4.2. From the results, the last experiment had the appropriate condition for forming. The green strength of the specimen was strong enough to resist deformation due to its own weight and the visual appearance was smooth and had good symmetry.

Table 4.2 Conditions for extruded HAp specimens

Condition	PVA %	Dispex %	Glycerine %	Moisture %	Pressure (Kg/cm^2)	Bulk density of sintered HAp g/cm^3	Result
1	2	0.5	-	20	160	2.75	√
2	2	0.5	-	25	160	2.82	√
3	3	0.5	-	20	100	2.51	X
4	3	0.5	-	23	75	2.49	X
5	3	0.5	-	25	75	2.44	√
6	2	0.5	-	23	75	2.54	√
7	2	0.5	2	16	75	2.34	X
8	2	0.5	3	17	75	2.38	X
9	2	0.5	5	21	100	2.48	X
10	2	0.5	4	15	100	2.53	√
11	2	0.5	5	18	100	2.81	*
12	2	0.5	5	15	100	2.87	*

√: able to form X : unable to form √ * : improved by blending and be able to form

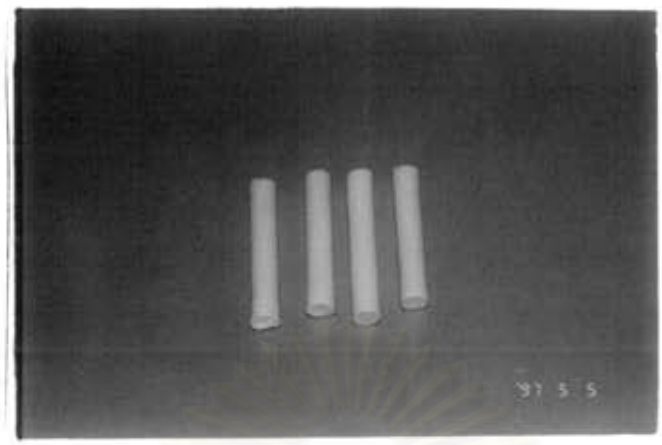

Fig.4.2 Sintered HAp specimens

4.2.2 Characteristics of Sintered Hydroxyapatite Specimens

4.2.2.1 Phase Identification

The XRD pattern of sintered HAp at 1250 °C as shown in Fig. 4.3 indicated that the second phase of the sintered HAp was absent.

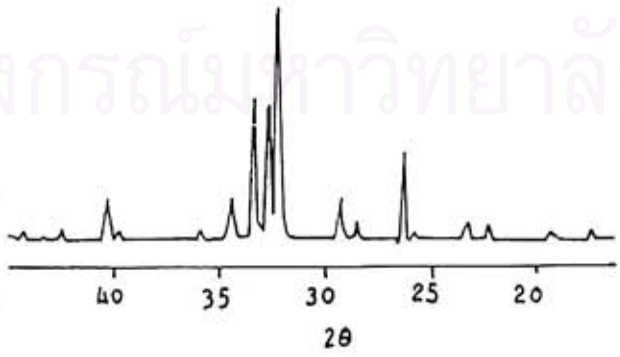

Fig. 4.3 XRD pattern of HAp specimen

4.2.2.2 Microstructure

Fracture surface of sintered HAp was shown in Fig.4.4. There was no significant increase in grain growth of HAp at 1250 °C but only pore size was decreased.

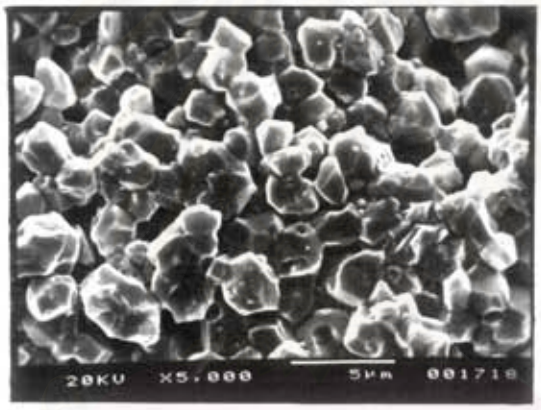

Fig. 4.4 SEM of HAp specimens

4.2.2.3 Properties of Sintered HAp

The water absorption, apparent porosity, bulk density and relative density of the sintered HAp were shown in Table 4.3. The results showed that the extrusion process could not prepare high density specimen but it was a common process for a suitable object with high symmetry.

Table 4.3 Properties of sintered HAp

Properties	HAp specimens
Water absorption, %	1.87
Apparent porosity, %	5.39
Bulk density, g/cm^3	2.87
Relative density, %	90.82

* Theoretical density of HAp = 3.16 g/cm^3

4.3 Mechanical Strength of Sintered Hydroxyapatite

The compressive strength and flexural strength of sintered HAp at 1250° C were shown in Table 4.4.

Table 4.4 Compressive strength and flexural strength of sintered HAp

Specimen	Compressive strength, (MPa)	Flexural strength, (MPa)
Sintered HAp	188±23	27±5

4.4 Characteristic of Calcium Phosphate Glass

After, melting and forming in a graphite mold, it was seen that the glass specimens were clear appearent but poor durability resistance. Moreover, they were susceptible to cracking so that annealing was required at temperature about 20 °C higher than the T_g of each CP glass . Finally, the specimens were cut and thermal expansion was determined by a dilatometer. The result was shown in Table 4.5.

Table 4.5 Thermal expansion and glass transition temperature of CP glass

Composition	mole of Na_2O added in CP glass	Thermal expansion, α ($\times 10^{-6}$ K^{-1})	T_g ($^{\circ}C$)
C1	0.02	11.3	490
C2	0.03	11.7	488
C3	0.04	11.9	474
C4	0.10	13.0	452
C5	0.15	14.2	426
C6	0.18	15.0	418
C7	0.20	15.3	414

* Thermal expansion coefficient of HAp (27- 450 °C) 15.7×10^{-6} K^{-1}

The data shown in Table 4.5 indicate that thermal expansion was increased with amount of Na_2O added. Therefore , calcium phosphate glass can be produced to possess the required thermal expansion. Moreover, the stable calcium phosphate glass can be also produced using the Tg values. The variation of thermal expansion coefficient for calcium phosphate glass with amount of mole Na_2O added are presented graphically in Fig. 4.5.

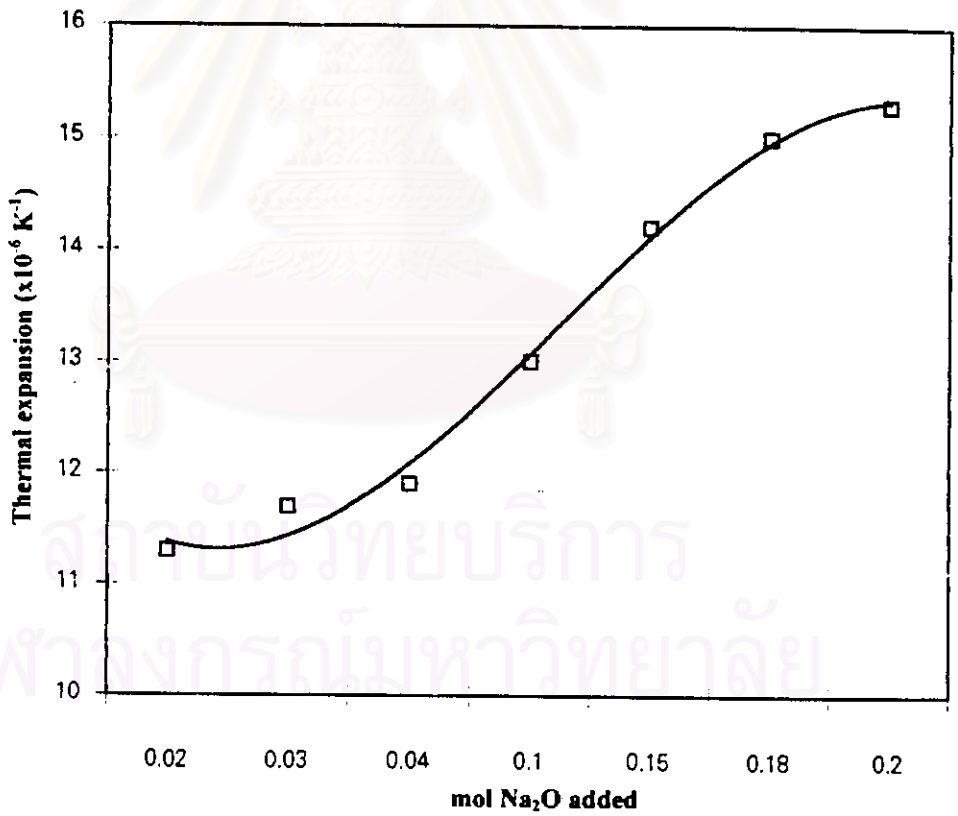

Fig. 4.5 Change of thermal expansion coefficient as a function of mol Na_2O .

Table 4.6 Difference of thermal expansion coefficient between HAp and CP glass

HAp sample	Δ Thermal expansion coefficient ($\times 10^{-6}$ K^{-1})
HAp-C1	4.4
HAp-C2	4.0
HAp-C3	3.8
HAp-C4	2.7
HAp-C5	1.5
HAp-C6	0.7
HAp-C7	0.4

Calcium phosphate glass with composition of C4, C5 and C6 were selected to coat on HAp because they had the suitable difference of thermal expansion coefficient to induce compressive surface stress. The difference of thermal expansion coefficient of HAp compared with calcium phosphate glass was shown in Fig.4.6 - 4.8.

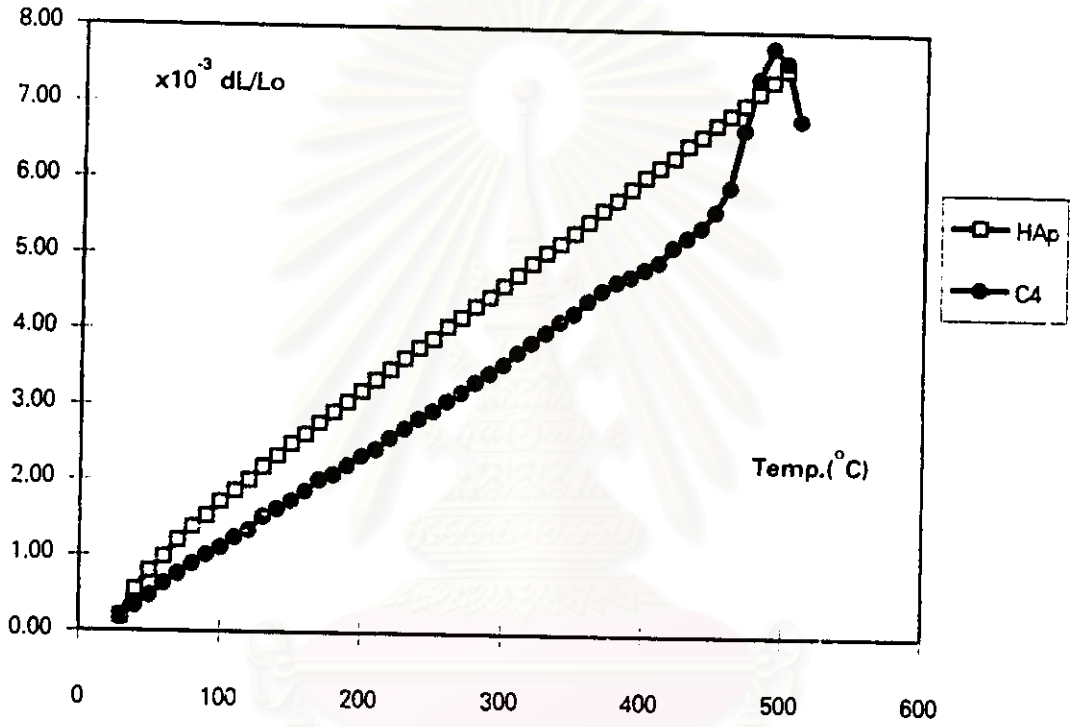

Fig.4.6 The variation of thermal expansion coefficient of HAp compared with C4.

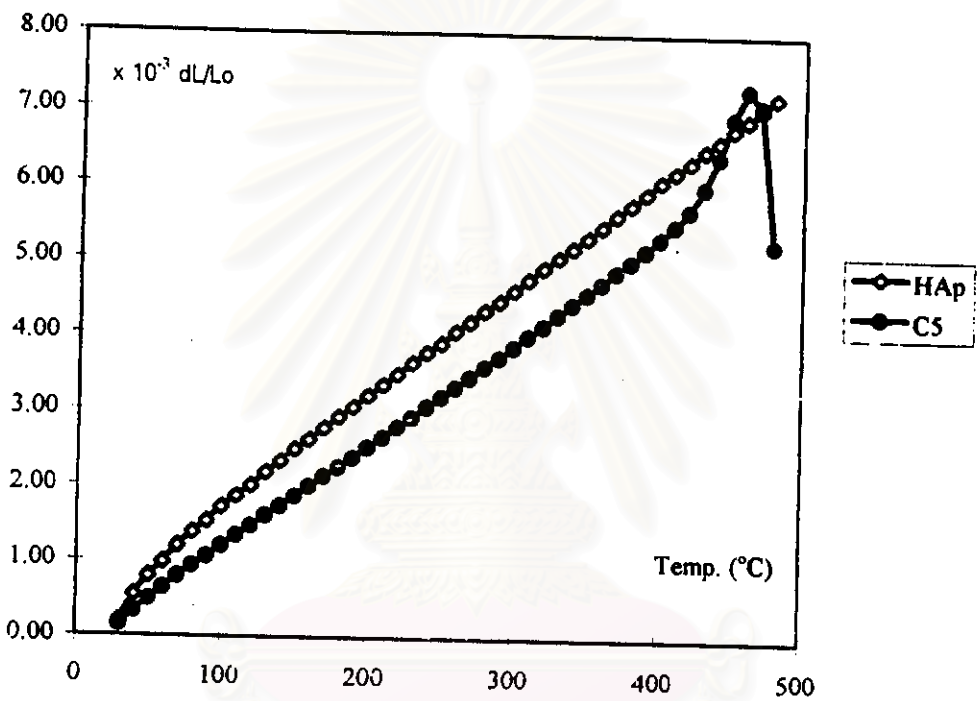

Fig.4.7 The variation of thermal expansion coefficient of HAp compared with C5.

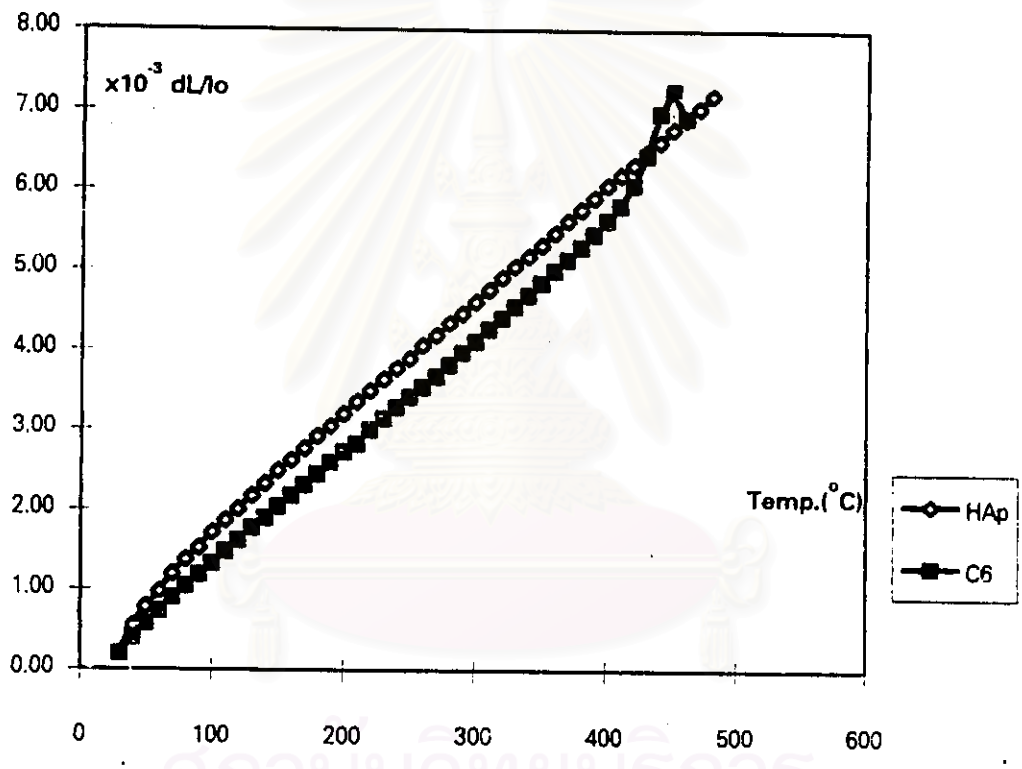

Fig.4.8 The variation of thermal expansion coefficient of HAp compared with C6.

Coated HAp specimens were prepared by dipping hot sintered HAp into the molten glass at 1100° C, then allowed specimens to cool in oven. At higher temperature corresponding to T_g of CP glass, CP glass could flow and cover throughout the specimen. When the temperature was decreased down to the temperature at the intercept of thermal expansion of HAp and CP glass. Compressive stress was induced by the difference of thermal expansion.

4.5 Characteristic of Coated HAp

Coated HAp was obtained by dipping sintered HAp specimen into the molten glass. After coating, the coated HAp was kept in two conditions, one annealing at a temperature higher than T_g of CP glass and another, allowing to gradually cool in furnace.

The surface appearance of coated specimens with annealing was smooth and clear. Moreover, there were no crystallinity and cracking appeared in the specimen. Whereas the rough surface was found in the specimen which was not annealed, the average thickness of the coating layer are lower than that of HAp specimens obtained under annealing condition and crystal region also existed. The appearance of the specimen obtained from the above two conditions were illustrated in Fig.4.9 and Fig. 4.10.

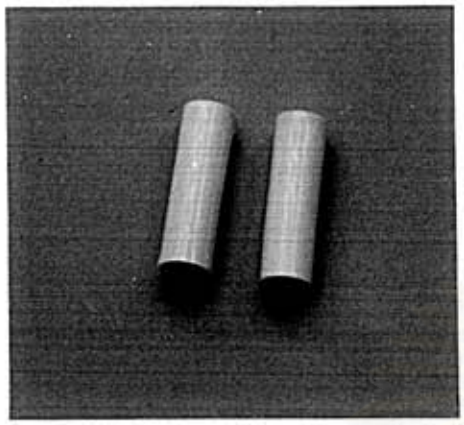

Fig.4.9 Coated HAp under annealing

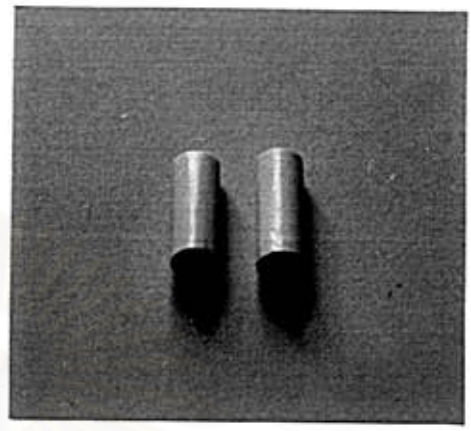

Fig.4.10 Coated HAp without annealing

4.5.1 Thickness

The thickness of the coating layer was determined by scanning electron microscopy as tabulated in Table 4.7. The thickness of coated HAp under annealing was higher than that of coat HAp without annealing. This is a result from the preparation of coated HAp under annealing was kept immediately at annealing temperature about 450° C after dipping whereas coated HAp without annealing was kept at slightly higher location than dipping location which had higher annealing temperature in gradient furnace. The higher temperature could lead CP glass to easier flow in free stress state. The resulting specimen had the thinner layer with a comparison to the specimen which was kept at annealing temperature . However, the thickness of specimen was controlled difficultly because of the limited dimension of furnace.

Table 4.7 Thickness of coated HAp specimens.

Coated HAp	Thickness (μm)
under annealing	
HAp-C4	165 ± 15
HAp-C5	150 ± 10
without annealing	
HAp-C4	105 ± 16
HAp-C5	65 ± 12
HAp-C6	55 ± 13

4.5.2 Microstructure

The microstructures of the coated HAp observed by a scannning electron microscope were shown in Fig.4.11 and Fig. 4.12

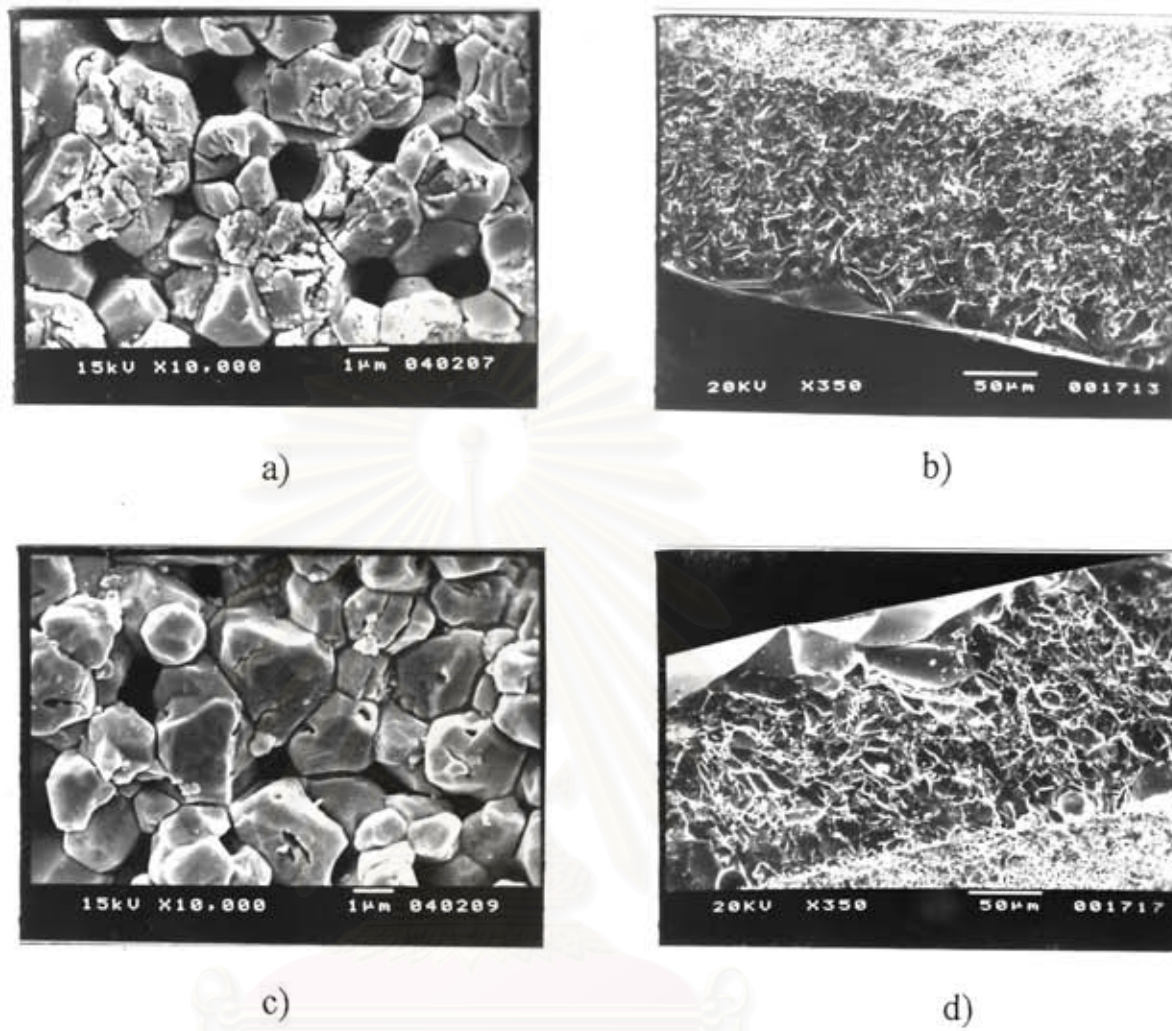

Fig.4.11 Microstructure of coated HAp under annealing

a), b) HAp - C4 c), d) HAp - C5

Fig.4.11 a). presented microstructure of substrate of coated HAp with CP glass composition C4 (HAp - C4). Cracking was appeared in particle which was expected to affect by thermal shock while the specimen was moved immediately from dipping temperature at 1100° C to annealing temperature 450° C.

Fig. 4.11 b) presented the microstructure at the interface of HAp-C4. The porosity of HAp substrate at interface was decreased by CP glass diffusion to the HAp substrate .

Fig. 4.11 c) presented microstructure of substrate of coated HAp with CP glass composition C5 (HAp - C5). The crack was also found as in the HAp-C4 specimen since two substrates were coated by the same condition.

Fig. 4.11 d) presented the microstructure at the interface of HAp-C5. The diffusion of CP glass into the pore of HAp substrate was also found as in HAp-C4.

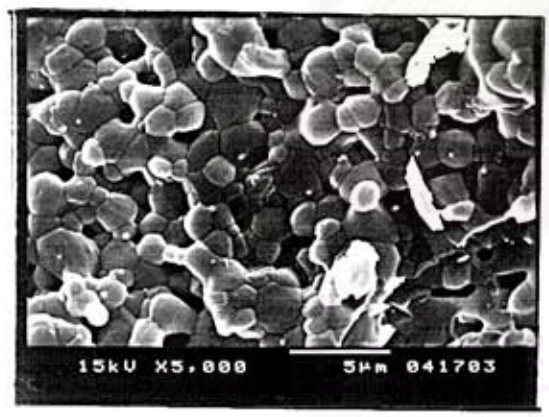

a)

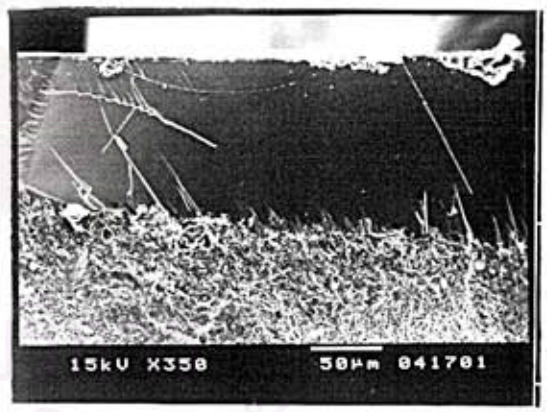

b)

Fig. 4.12 Microsturcture of coated HAp without annealing

a), b) HAp - C4

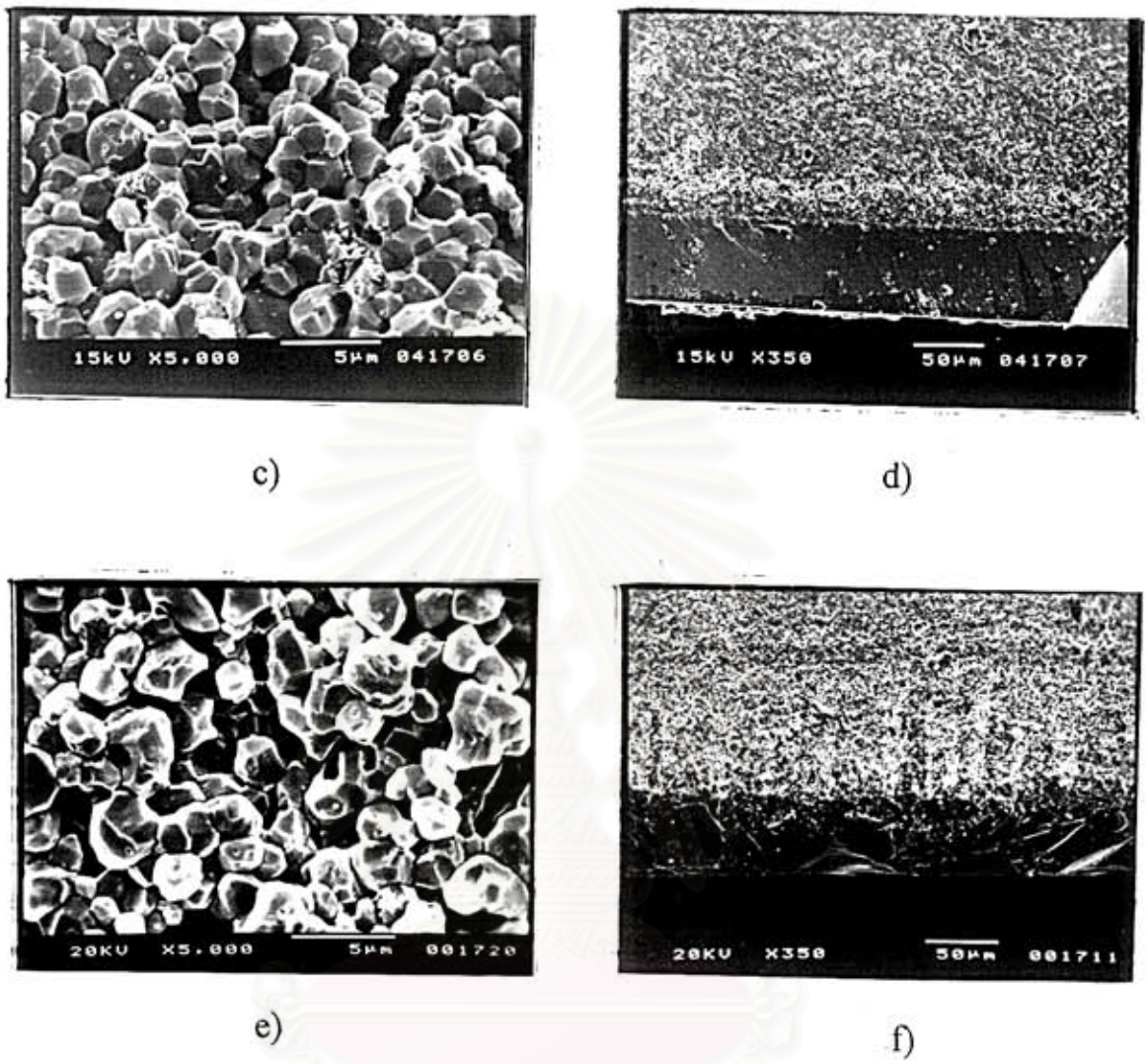

Fig. 4.12 Microsturcture of coated HAp without annealing
c), d) HAp - C5 e), f) HAp - C6

Fig 4.12 a, c and e shown the microtructure of HAp substrate which was coated with calcium phosphate glass composition C4, C5 and C6, respectively. It was found that the pore was remained in substrate because the substrate was formed by extrusion process. In the present study could prepared to 90% theoretical density of HAp at 1250°C and was without microcrack in grains.

Fig 4.12 b, d and f were shown the microstructure of coated HAp at interfaces which were coated with calcium phosphate glass composition C4, C5 and C6, respectively. There was diffusion of molten glass to fill into HAp substrate. The thickness of coating layer was lower than specimen under annealing, resulting in the higher induction of compressive surace stress.

4.6 Strength Measurement of Coated Hydroxyapatite

The compressive strength of coated HAp (with C4, C5 and C6) was shown in Table 4.8

Table 4.8 Compressive strength of coated HAp under annealing

Coated HAp	Compressive Strength (MPa)
HAp-C4	126 ± 13
HAp-C5	112 ± 14
uncoated HAp	188 ± 23

Compressive strength of coated HAp under annealing was decreased with a comparison to uncoated HAp. The microcrack was developed in particle as shown in Fig 4.11, although CP glass diffused to fill into the pore at the interface of the substrate. This is the result of the high difference of temperature, the thermal shock was occurred while coated spacimen was transfered from dipping temperature to

annealing temperature. In addition, the annealing process could eliminate stress which reduced the induction of compressive stress at surface, leading to the decrease of strength.

Table 4.9 Flexural strength of coated HAp without annealing

Coated HAp	Flexural Strength (MPa)
HAp-C4	28 ± 2
HAp-C5	29 ± 2
HAp-C6	32 ± 3
uncoated HAp	27 ± 5

The flexural strength of coated HAp without annealing was increased to 3.7%, 7.4% and 18.5% for coating with calcium phosphate glass had composition C4, C5 and C6, respectively, as seen in Table 4.9. The strength of coated HAp was increased due to the filling of molten glass into the pore of HAp substrate and the thickness of coated layer was adequate to induce compressive surface stress. It was found that the increased thickness resulted in decreasing of strength (Sumalee, 1996). Moreover, coated specimens were not transfered from dipping temperature to annealing temperature after annealing.

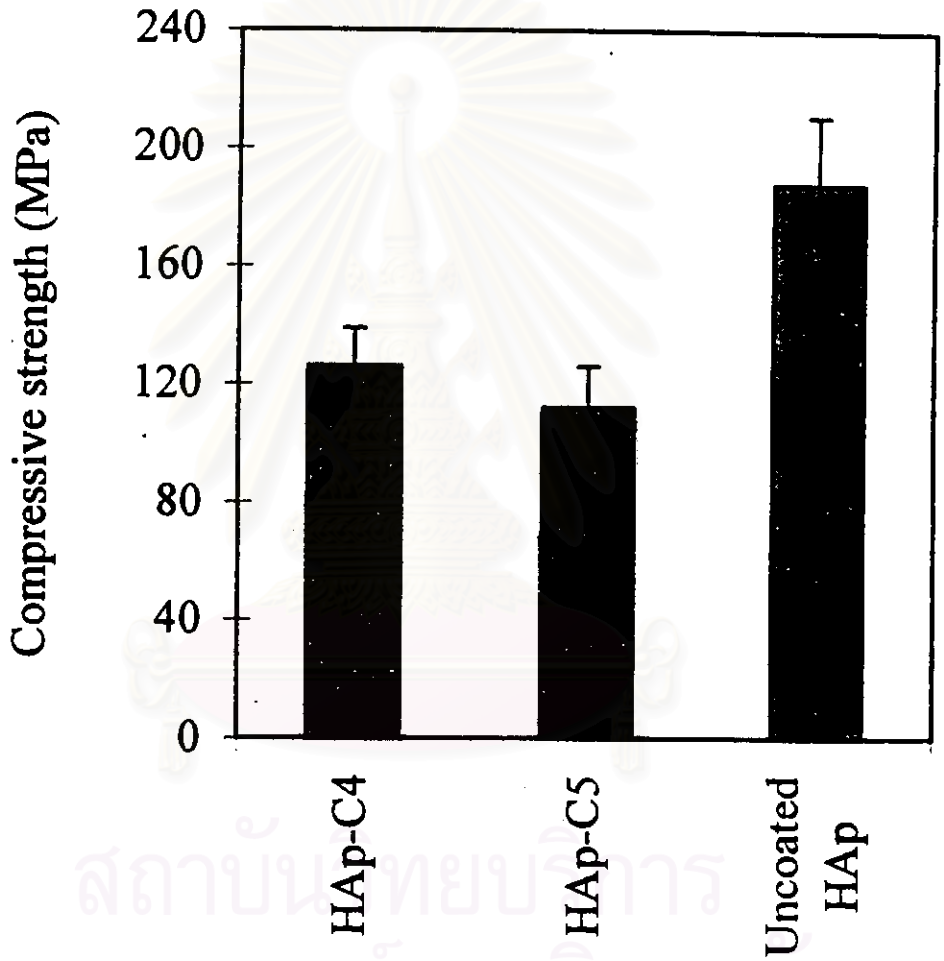

Fig 4.13 The comparison of compressive strength of uncoated HAp and coated with C4 and C5 under annealing

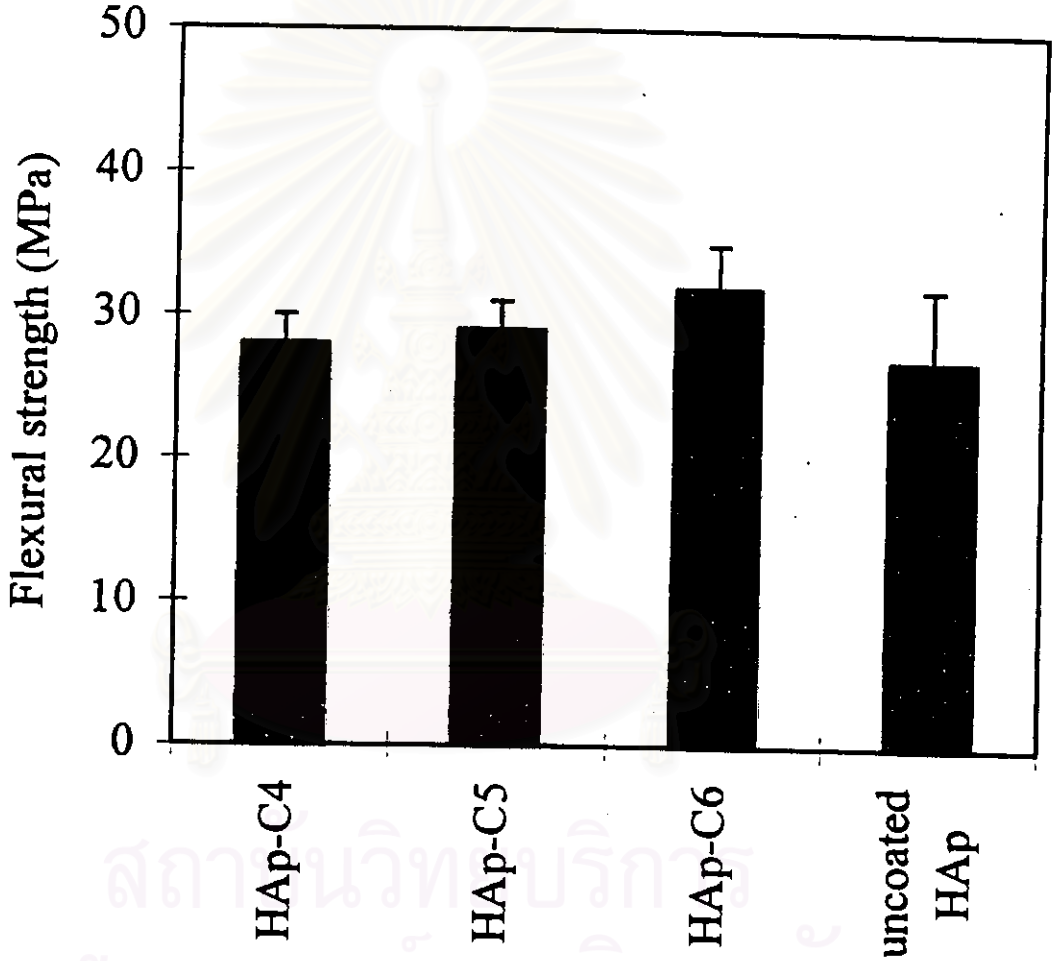

Fig.4.14 The comparison of flexural strength of uncoated HAp and coated HAp with C4, C5 and C6 without annealing